Heterogeneous Composition and Microstructure of Elastomeric Polypropylene from a Sterically Hindered 2-Arylindenylhafnium Catalyst

Willy Wiyatno,[‡] Zhong-Ren Chen,[†] Yuxiang Liu,[†] Robert M. Waymouth,*[,†] Val Krukonis,[§] and Kara Brennan[§]

Departments of Chemistry and Chemical Engineering, Stanford University, Stanford, California 94305-5080, and Phasex Corporation, 360 Merrimack Street, Lawrence, Massachusetts 01843

Received March 4, 2002; Revised Manuscript Received November 11, 2003

ABSTRACT: The metallocene catalyst bis(2-(3,5-di-*tert*-butylphenyl)indenyl)hafnium dichloride yields elastomeric polypropylene in the presence of a MAO cocatalyst at 50 °C in liquid propylene. The polymer synthesized has M_w = 201 000 and narrow polydispersity (M_w/M_n = 2.3) with an average isotacticity [mmmm] = 34%. Several methods of fractionations were carried out to investigate the heterogeneity of the elastomeric polypropylene: thermal fractionation by DSC, boiling-solvent extraction, supercritical fluid fractionation employing increasing pressure profiling (IPP), and critical isobaric temperature rising elution fractionation (CITREF). Thermal fractionation reveals a distribution of crystallizable fractions with several melting points between 40 and 100 °C and a large melting endotherm at 150 °C which is attributed to the presence of long crystallizable segments. Fractionation by boiling-solvent extraction separates the elastomeric polypropylene into three fractions where the molecular weight, tacticity, and crystallinity increase in the following order: ether-soluble < heptane-soluble < heptane-insoluble fractions. Supercritical fluid fractionations by either molecular weight (IPP) or crystallinity (CITREF) show that the tacticities, melting points, and heats of fusion increase gradually with increasing molecular weight.

Introduction

The remarkable pace of developments in the application of well-defined coordination compounds in polymerization catalysis has advanced our understanding of the mechanistic details of olefin enchainment,[1−3] illuminated many of aspects of the structure property relationships of polyolefins,[4,5] and has led to the introduction of new classes of polyolefins with improved properties.[3] In the past few years, new classes of polyolefin elastomers (POE) have been introduced on a commercial scale.[3] The elastomeric properties of these materials are a consequence of the lower densities and crystallinities compared to the corresponding thermoplastics. For polyethylene elastomers, these advances were made possible by new catalysts capable of incorporating comonomers randomly and homogeneously into the polyethylene backbone to give polymers with narrow molecular weight and composition distributions. The physical properties of these polyolefin elastomers are in some cases competitive to conventional elastomers and the efficiency of polyolefin production and processing allows them to be produced at a competitive cost/performance ratio.[3]

Polyolefin elastomers derived from propylene have also been long investigated.[6−17] The higher-melting points of polyolefins derived from propylene is an advantage for high-temperature applications, although the high glass transition temperatures of polypropylenes limits their low-temperature applications. Polypropylene elastomers were first reported by Natta, who was the first to propose that the elastomeric properties of these materials were a consequence of a stereoblock structure consisting of alternating runs of crystalline isotactic and amorphous atactic diastereosequences.[6−10] After Natta's work, there have been a number of efforts to improve the selectivity of catalyst systems for the production of elastomeric polypropylenes with notable advances by Collette and co-workers at Dupont[11−16] and Job at Shell.[17] More recently, several classes of metallocene catalysts have been developed for the production of elastomeric polypropylenes,[18−26] notably those developed by Chien,[27−31] Collins,[32−34] Rieger,[35,36] Pellon,[37] and our group.[21,38−70] As for the polyethylene-derived polyolefin elastomers,[71−73] potential advantages of metallocene catalysts are the ability to tailor the structures and properties of the propylene elastomers by suitable modifications of the coordination catalyst precursors.

We have previously reported that conformationally dynamic unbridged metallocenes based on bis(2-arylindenyl)metallocene catalyst systems yield polypropylene elastomers.[38−59] The structures and properties of these materials differ from both those produced with heterogeneous catalysts and those produced with the bridged metallocene catalysts. These materials exhibit broad melting ranges and high-melting points typical of the materials produced from heterogeneous catalysts[11] but possess narrower molecular weight distributions typical of metallocene polymers. Nevertheless, the molecular weight distributions are slightly broader and the melting points of the polypropylene elastomers produced from the bis(2-arylindene)metallocene catalysts are higher than those produced from the C_1-symmetric metallocenes.[74] These polypropylenes have melting point ranges from 25 to 165 °C, similar to those produced with the heterogeneous catalysts.[11] In addition, the composition or tacticity distributions are broad, as they can be separated into fractions of different tacticities and crystallinities.[44,45,51−53,60,62]

[†] Department of Chemistry, Stanford University.
[‡] Department of Chemical Engineering, Stanford University.
[§] Phasex Corporation.

10.1021/ma020332j CCC: $27.50
Published on Web 01/03/2004

Table 1. Polymer Characterization

sample	wt %	M_w[a] (K)	PDI[a]	mmmm (%)[b]	m (%)[b]	IR index[c]	T_m (°C)[d]	ΔH (J/g)[d]	crystallinity (%) DSC	crystallinity (%) XRD
ePP-10	100	201	2.3	34	73	0.34	42−149	22	11	8
ePP-10 annealed							50−160	27	14	
ES-ePP10	48	147	2.1	21	67	0.19	41−45	2	1	2
HS-ePP10	42	220	2.3	44	79	0.38	42	32	15	11
HI-ePP10	10	432	2.5	76	92	0.70	47−155	82	39	37

[a] Determined by GPC (Waters, 150 °C) at BP Chemical Co. [b] Determined by ^{13}C NMR. [c] Determined by the ratio of absorbance intensity A_{998}/A_{975}. [d] Determined by DSC endotherm scan from 0 to 200 °C at 20 °C/min.

In this work, we report the compositional heterogeneity of elastomeric polypropylenes derived from the 2-arylindene metallocene bis(2-(3,5-di-*tert*-butylphenyl)-indenyl)hafnium dichloride.[75] The catalyst is a modification to that previously reported by our group through ligand substitution at the 3,5-positions and the use of a hafnium metal rather than zirconium.[44,45,51−53,62−64] The compositional hetereogeneity of these polypropylenes was investigated by a variety of techniques, including thermal DSC fractionation, boiling solvent extraction, and supercritical fluid fractionations. Analysis of the fractions was carried out by DSC, GPC, and ^{13}C NMR methods.

Results and Discussion

The elastomeric polypropylene investigated for this study was prepared with bis[2-(3,5-di-*tert*-butylphenyl)-indenyl]hafnium dichloride[75]/MAO at 50 °C in liquid propylene at BP Chemical Co. This material is very similar in average microstructure and properties to the elastomeric polypropylene PP1 we have previously reported[44,45,51−53] but was prepared with a different catalyst. We have previously shown that the structures and properties of elastomeric polypropylenes can be influenced by the nature of the arylindene ligand and the transition metal.[40] Introduction of *tert*-butyl substituents in the 3,5-positions of the 2-arylindenyl substituent results in higher tacticity polypropylenes relative to the unsubstituted derivatives,[50,58] and the hafnium derivatives yield lower tacticities than the zirconium derivatives.[40] Because of these two effects, the bis[2-(3,5-di-*tert*-butylphenyl)indenyl]hafnium dichloride/MAO catalyst system yields a similar polypropylene at 50 °C as the bis(2-phenylindenyl)zirconium dichloride/MAO catalyst system at 25 °C; an advantage of the *tert*-butyl-substituted hafnium metallocene is its ability to produce polypropylenes of appropriate molecular weight and tacticity at higher temperatures.[40,57] The polypropylene produced under these conditions (ePP-10) is a low-tacticity polypropylene ([mmmm] = 34%) of approximately 11% crystallinity with a density of 0.863 g/mL.[60,62−64,76] This material (ePP-10) has similar properties[62−64] but is of lower molecular weight (M_w = 201 000 vs 455 000) and has a slightly lower polydispersity (Table 1) than the elastomeric polypropylene PP1 produced with the bis(2-phenylindenyl)zirconium dichloride/MAO catalyst system at 25 °C.[44,45,51−53] As shown in Figure 1, ePP-10 has a broad melting transition, spanning 40−160 °C with peak melting points around 40 and 150 °C (Figure 1).[62]

The broad melting transition in this material is indicative of a broad distribution of crystallite sizes and stabilities. This broad melting range can be attributed to either a distribution of isotactic sequence lengths in the polymers or kinetic constraints in the crystallization process, or both. In an effort to distinguish these possibilities and to investigate the influence of thermal history on the properties of these materials, a sample of ePP-10 was annealed in a stepwise manner from 160 °C to room temperature in a vacuum oven over 10 days.[62,77] The heating trace of the annealed sample (Figure 1) exhibits several melting points, with a large endotherm at approximately 150 °C and several smaller peaks between 40 and 100 °C. Tensile measurements of both the annealed and compression-molded sample[62] reveal them to be elastomeric with comparable properties to those reported previously for samples of similar structure.[45,46] These properties are characteristic for this family of elastomeric polypropylenes for this range of isotacticities (25 ≤ [mmmm] ≤ 40).[74] The presence of the high-melting component is indicative of the presence of long isotactic sequences; the presence of lower-melting fractions would suggest a distribution of crystallite sizes, which could in turn be due to a distribution of isotactic sequence lengths in the polymer.

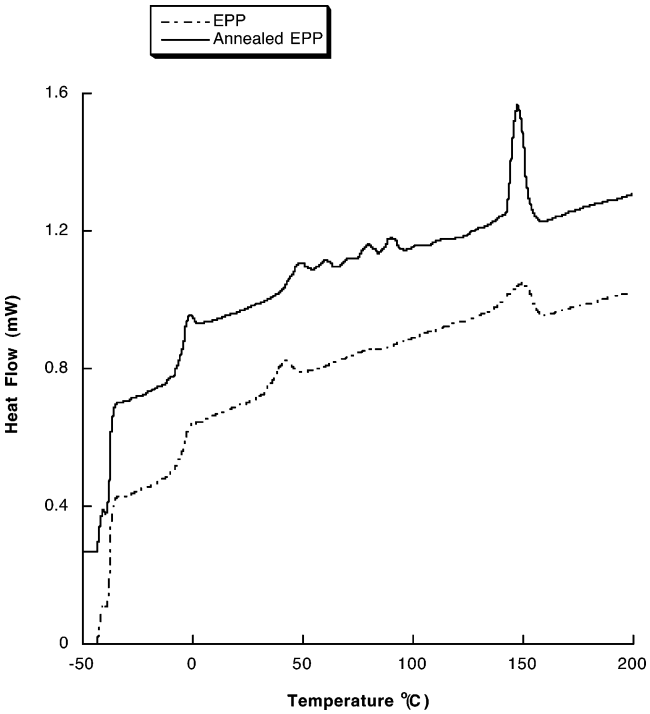

Figure 1. DSC thermal characterization of ePP-10 and annealed ePP-10.

Boiling Solvent Extraction. To characterize the compositional heterogeneity of these polypropylenes, fractionations in boiling solvents were carried out. As observed for PP1, the polypropylene homopolymer ePP-10 is heterogeneous and can be separated into several fractions which differ in their degree of tacticity, crystallinity, and solubility in different solvents.[44,45,51−53] Extraction of ePP-10 in boiling diethyl ether and heptane yielded three fractions as shown in Tables 1 and

Table 2. ^{13}C NMR Pentad Distribution of EPP and Its Solvent Fractions

sample	mmmm	mmmr	rmmr	mmrr	rmrr + mmrm	mrmr	rrrr	mrrr	mrrm
ePP-10	0.34	0.16	0.05	0.08	0.20	0.08	0.01	0.04	0.04
ES-ePP10	0.21	0.18	0.06	0.09	0.26	0.10	0.01	0.05	0.04
HS-ePP10	0.44	0.20	0.02	0.07	0.18	0.04	0.01	0.01	0.03
HI-ePP10	0.76	0.09	0.02	0.03	0.06	0.01	0.00	0.01	0.02
IPP-11	0.38	0.16	0.04	0.07	0.20	0.07	0.02	0.03	0.03
CT-A9	0.41	0.15	0.05	0.07	0.17	0.07	0.01	0.04	0.03

2: an ether-soluble (ES) fraction (48 wt %) of low tacticity ([mmmm] = 21%), a heptane-soluble (HS) fraction (42%) of intermediate tacticity ([mmmm] = 44%), and a heptane-insoluble (HI) fraction (10%) of relatively high tacticity ([mmmm] = 76%). The pentad distributions of ePP-10 and its fractions are listed Table 2. Infrared spectroscopy measurements of the ratio of A_{998}/A_{975} correlate with the percentage of isotactic pentads [mmmm]: ePP, ES, HS, and HI have A_{998}/A_{975} = 34%, 19%, 38%, and 70%, respectively. Solvent extraction also yields fractions differing in molecular weights. ES has the lowest M_w = 147K (M_w/M_n = 2.1), HS has M_w = 220K (M_w/M_n = 2.3) similar to the parent ePP with M_w = 201K (M_w/M_n = 2.3), and HI has the highest M_w = 432K (M_w/M_n = 2.5). Fractionation by this solvent extraction method appears to occur by both molecular weight and crystallinity as the molecular weight, tacticity, and crystallinity increase from the ether-soluble fraction to the heptane-insoluble fraction.

The fractionation experiments reveal that the distribution of crystallites, indicated by the DSC measurements, is at least partially due to compositional heterogeneity in these materials. This behavior is closely analogous to that previously reported by Collette and co-workers,[11,15] who showed that elastomeric polypropylenes prepared from supported zirconium and titanium complexes could be fractionated into ES, HS, and HI fractions. Molecular weight distributions of Collette's samples were broad; the ether-soluble fraction in particular had polydispersities ranging from M_w/M_n = 7.5 to M_w/M_n = 11.7.[11,15] In contrast, the molecular weight distributions of ePP-10 and its fractions are narrower, in the range $2.1 \le M_w/M_n \le 2.5$. This unusual combination of narrow molecular weight distributions and broad composition distributions prompted us to carry out additional fractionation experiments using supercritical fluids.

Supercritical Fluid Fractionation. Supercritical fluid separation provides two complementary techniques for fractionating polymers: isothermal increasing pressure profiling (IPP), which fractionates polymers by molecular weight, and critical isobaric temperature rising elution fractionation (CITREF), which separates polymers by crystallinity.[78,79] Increasing pressure profiling (IPP)[79] is is carried out by distributing a sample of polymer powder on a knitted stainless steel mesh support and placing this sample into a pressure vessel. The polymer was dissolved in a supercritical fluid at high pressure and temperature (typically 700 bar and 150 °C) and then deposited onto the support by lowering temperature and pressure simultaneously. Fractionation was carried out using supercritical ethane at 140 °C (which was known to dissolve ePP-10). The solubility of polymer in the melt is molecular weight and pressure dependent, and fractions of increasing molecular weight were collected by raising the pressure stepwise from 100 bar for the low molecular weight fraction to 700 bar to dissolve the high molecular weight chains. In this molecular weight fractionation, 96.6% of feed weight

Table 3. Characterization of Increasing Pressure Profiling (IPP) Separation Fractions

sample ID	wt %	mmmm (%)	M_w (K)	PDI	T_m range (°C)	ΔH (J/g)
IPP-1	1.7					
IPP-2	5.7		96.6	27.2	45−135	8.8
IPP-3	6.7		55.3	1.6		
IPP-4	13.2	33	93.5	1.56	40−155	16.5
IPP-5	14.1		102	1.5	40−155	16.7
IPP-6	3.3		135	1.4	40−155	16.7
IPP-7	20	34	188	1.41	40−155	16.2
IPP-8	2.5				40−155	20.8
IPP-9	12.9	35	201	1.4	40−158	26.1
IPP-10	5.9		303	1.5	40−160	29.1
IPP-11	9.8	38	400	1.63	40−155	30.5
IPP-12	3.8		358	2.1	40−160	37.6

was recovered from the column in 12 fractions. Representative fractions were analyzed by GPC, ^{13}C NMR, and DSC as reported in Table 3. The GPC trace of one of the early fractions, fraction 2 (approximately 6% of the sample), is trimodal with peaks at M_w of 740, 22 000, and 160 000 in relative areas of 1:2:2, respectively. Other remaining fractions yield monomodal GPC traces with narrow molecular weight distributions ($1.4 \le M_w/M_n \le 1.6$). As expected, the molecular weights increase with increasing elution pressure. Analysis of the microstructure of the various fractions by ^{13}C NMR reveals only a slight increase in tacticity with increasing molecular weight (fraction number), but the range is small ([mmmm] = 33−38%). DSC analysis of the fractions reveals similar broad melting endotherms with melting ranges from 40 to 160 °C for fractions IPP-2−IPP-12. A clear observable trend is the increase in heats of fusion with increasing molecular weight (fractionation pressure). Results from this fractionation appear to indicate that there is not a discontinuous change in the structure or crystallinity of the polymers over the molecular weight range, but a modest and gradual increase in the tacticity and crystallinity with increasing molecular weight.

Fractionation by supercritical temperature rising elution chromatography CITREF[78,79] in propane was also carried out. Two replicate fractionations were carried out for ePP-10 (Table 4) at 240 bar with a stepwise increase in temperature. In the first fractionation, nine fractions were recovered (100%) at temperatures between 40 and 120 °C. In the second fractionation at temperatures ranging from 20 to 110 °C, 99.6% was recovered in nine fractions.

Analysis of representative fractions (Table 4) is consistent with the picture from the IPP fractionation, that the tacticity and crystallinity of these polymers increase with increasing molecular weight. The molecular weight distributions of the CITREF fractions are narrow and only slightly broader than the pressure fractions (IPP method). The molecular weights of CT-A3 and -A6 are similar at M_w = 160 000, whereas that of CT-A9 is higher at M_w = 239 000. For CITREF fractionation, the isotacticities increase with increasing temperature (fraction number) and range from [mmmm]

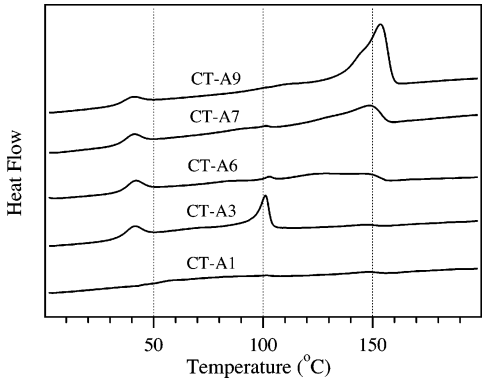

Figure 2. DSC thermal characterization of CITREF fractions.

Table 4. Characterization of CITREF Separation Fractions

fraction	temperature (°C)	wt %	mmmm (%)	M_w (K)	PDI	T_m range (°C)	ΔH (J/g)
CT-A1	40	31.2	28	165	2.0	40−155	12.9
CT-A2	40	7.8					
CT-A3	40−50	7.8	30	150	1.8	40−115	12.2
CT-A4	50−60	8.5					
CT-A5	60−70	6.9					
CT-A6	70−80	11.1	35	160	2.0	40−155	22.9
CT-A7	80−90	12.7	35			40−159	22.3
CT-A8	90−100	3.9					
CT-A9	100−120	10.1	41	239	2.3	40−162	38.1
CT-B1	20	10.2	25			25−154	7.1
CT-B2	50−60	14.8	36			25−161	26.9
CT-B3	90−100	15	40			25−161	33.4
CT-B4	100−110	3.8	49			25−164	44.8

= 28% for CT-A1 to [mmmm] = 41% for CT-A9. Reproducibility of this fractionation method was checked by a second CITREF fractionation and yielded a material balance of 99.6%; the final fraction of this run (3.8% of the sample) has the highest tacticity with an [mmmm] = 49%. As with the pressure fractionation, DSC analysis reveals similar broad melting endotherms for all fractions with a consistent increase in the heat of fusion with increasing elution temperature as shown in Figure 2.

A larger range of compositions is evident from the CITREF fractionation than from the IPP fractionation. The tacticities of the fractions range from [mmmm] = 28% for CT-A1 to [mmmm] = 41% for CT-A9, and the total crystallinity of the fractions increases with increasing elution temperature. DSC endotherm curves of fractions CT-A3 through CT-A9 reveal broad and bimodal melting curves where the high-melting peak shifts from approximately 100 °C for fraction CT-A3 to 155 °C for CT-A9.

Surprisingly, neither the IPP fractionation nor the CITREF fractionation gives any obvious evidence for the HI fraction obtained from the solvent extraction. The absence of a highly tactic fraction in the supercritical fractionations is not well understood. We have carried out solvent fractionation of this sample multiple times with good reproducibility to isolate 10% HI with isotacticity [mmmm] = 76%. There are two possible explanations: (1) in the supercritical fractionation the high molecular weight, more isotactic components are degraded and/or not eluted or (2) that the mechanism of fractionation using boiling solvent and supercritical fluid is sufficiently different that the HI fraction observed by solvent extraction is not separated in the supercritical fractionation technique and is distributed among the other fractions of the sample. Material

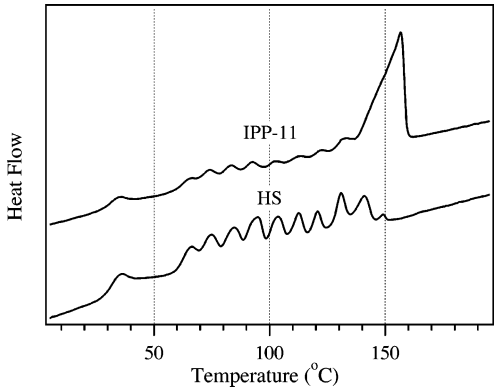

Figure 3. Thermal fractionation investigated by DSC of the intermediate-tacticity heptane-soluble (HS-ePP10) fraction and the supercritical fluid fraction IPP-11.

balances of these fractionations reveal that almost all of the sample is recovered: in the IPP fractionation, 96.6% of the polymer is recovered; in the CITREF fractionations, 100% and 99.6% of the samples are recovered. The fact that we observe a trimodal molecular weight distribution for an early IPP fraction (IPP-2) may be indicative of some decomposition of the polymer sample under the fractionation conditions; nevertheless, the combined amounts of fractions IPP-1 and IPP-2 constitute only 7.4% of the whole sample.

At present, we do not have an unambiguous explanation for the failure of the supercritical fluid fractionation to isolate the HI fraction. It may be related to the observation that these polymers are unusual in that they are reasonably homogeneous in terms of molecular weight distribution but have broad composition distributions. As the fractionation procedures are likely to occur by different mechanisms, it would appear that the solvent fractionation method is better able to isolate the high-crystallinity fractions. Our results indicate that no single fractionation technique is sufficient to provide a complete picture of the heterogeneity and composition of these materials and that all three (solvent fractionation, IPP fractionation, and CITREF) provide useful information.

To further characterize the properties of the fractions of ePP, thermal fractionation DSC was carried out on the heptane-soluble fraction HS-ePP10 and one of the supercritical fractions obtained from the pressure fractionation (IPP-11).[77] These samples have reasonably similar microstructures as revealed by ^{13}C NMR pentad distributions (HS [mmmm] = 44%, IPP-11 [mmmm] = 38%; Tables 2 and 3) and narrow molecular weight distributions, but the IPP-11 fraction is of higher molecular weight. Thermal fractionation was carried out by cooling a DSC sample in a stepwise manner from 160 to 50 °C at 10 °C intervals, each annealed for 12 h. DSC thermal fractionation traces of these two samples are shown in Figure 3. Despite the similar tacticities as measured by ^{13}C NMR, the results of thermal fractionation of the two samples are quite different. While both samples reveal a series of melting peaks which span a broad temperature range, the DSC of sample IPP-11 is dominated by a large endotherm (ΔH approximately 15.5 J/g) at 158 °C, suggesting that this fraction has a larger number of longer, high-melting isotactic sequences.

Implications of the Fractionation/Thermal Analysis on the Microstructure of Elastomeric Polypropylene. The elastomeric properties of these polyprop-

ylenes are due to the presence of stereodefects or sequences of stereodefects in the chains that lower the crystallinity and provide amorphous sequences that can be oriented under an application of a deformation. Fractionation experiments reveal that these polypropylenes are a mixture of polymer chains with a distribution of isotacticities. These results suggest that the distribution of stereodefects is intramolecular (within the polymer chains), intermolecular (existing in mixtures of chains), or both. The fact that ePP-10 can be fractionated clearly establishes that there is an intermolecular distribution of stereodefects. Results from the IPP supercritical fractionations imply that this distribution of stereodefects is not strongly segregated by molecular weight, but rather there is a gradual decrease in the total number of stereodefects with increasing molecular weight (as manifested by the increase in [mmmm] with increasing M_w).

Analysis of the thermal properties of ePP-10 and the individual fractions has provided some insight into the microstructure of the polypropylenes and the broad melting transitions characteristic of this class of polypropylenes. The broad melting transitions provide evidence for a distribution of crystallite stabilities in these materials, which are likely reflective of a distribution of crystallite sizes. The fact that the fractions also exhibit broad melting ranges (cf. Figures 2, 3 and Tables 1, 3, and 4) indicates that the narrow molecular weight fractions also contain a broad distribution of crystallite sizes when crystallized from the melt. This result implies that there is a distribution of isotactic sequence lengths even for polymer chains of similar molecular weight. This is consistent with an isotactic stereoblock structure containing a distribution of isotactic sequence lengths in a given chain. In particular, analysis of HS-ePP10 ([mmmm] = 44%, M_w/M_n = 2.3) by thermal fractionation DSC revealed a broad melting transition from 38 to 153 °C with a series of melting peaks from 60 to 150 °C (Figure 3). The presence of high-melting peaks in these fractions provides indirect evidence for long crystallizable isotactic sequences while the solubility in heptane and diethyl ether implies that these long isotactic sequences are chemically attached to amorphous sequences. Similar analysis of IPP-11, a fraction having a narrow polydispersity obtained from supercritical fractionation ([mmmm] = 38%, M_w/M_n = 1.6), revealed a large melting endotherm at 157 °C and several lower-melting peaks between 60 and 140 °C.

The high-melting peaks for these low-crystallinity polypropylenes can be compared to other low-crystallinity polypropylenes which show much lower-melting points. Balboni et al. synthesized polypropylene with C_2-symmetric zirconocenes catalyst *rac*-H_2C(3-*i*Pr-1-Ind)$_2$-$ZrCl_2$−MAO that yielded a low-tacticity elastomeric polypropylene with M_w = 143 700 and [mmmm] = 35%.[80,81] Although the isotacticity [mmmm] of this sample is similar to ePP-10, IPP-11, and HS-ePP10, the melting point of this sample was only 45 °C, and the polymer was completely soluble in boiling diethyl ether. These differences in the melting behavior are consistent with a different distribution of stereodefects in the chain where the lower-melting polypropylenes contain a random distribution of stereodefects and the higher-melting polypropylenes have a blocky distribution of stereodefects. The distribution of stereodefects and quantitative determinations of the length of isotactic and atactic stereosequences are difficult to establish since ^{13}C NMR provides only average estimates of these quantities. Analysis of the microstructure of HS-ePP10 and IPP-11 by ^{13}C NMR at pentad resolution is more consistent with an isotactic stereoblock polymer containing both isolated [mrmm] stereoerrors and blocks of atactic stereosequences (Table 2),[82] but experiments at higher resolution are warranted.[65−68,83]

Implications on the Polymerization Mechanism. The compositional heterogeneity of polypropylenes derived from 2-arylindene metallocene catalysts suggests that different catalyst sites are contributing to the polymerization process. The relatively narrow molecular weight distributions observed would require that all catalysts share similar propagation and chain-transfer characteristics. We attribute the compositional heterogeneity, narrow molecular weight distributions, and the observed concentration-dependent stereochemistry of ePP to a family of catalyst sites of different dynamics that are generated in the presence of cocatalyst MAO. Studies in our group and Busico's group have recently shown that the nature of the counterion can have a significant influence on the stereoselectivity of these catalysts.[58,59,66,68] The indeterminate structure of MAO may lead to a distribution of ion pairs with different dynamics; Busico has recently posited that some fraction of the catalyst sites are "locked" into stereoselective conformations, leading to some fractions of the polymer sample that are more highly isotactic.[68] The observed increase in tacticity with increasing monomer concentration reveals a process or processes that compete with the stereo-differentiating olefin insertion step; thus, some fractions of these sites are not "locked" and clearly have dynamics which manifest themselves in a differential rate of insertion and isomerization. The compositional heterogeneity would then be a consequence of different populations of dynamic catalysts present in the system.

We have previously proposed a simplified conformational dynamics of unbridged 2-phenylindene metallocenes which provides at least two types of sites, isospecific *rac* and aspecific *meso* configurations, that can interconvert during the polymerization process.[38,74] For the more sterically hindered *tert*-butyl-substituted 2-arylindene catalysts, other studies indicate that the achiral *meso* isomer is not likely to contribute to the polymerization behavior, leading to a significant fraction of isotactic stereoblock sequences separated by [mrmm] stereojunctions (Scheme 1).[58,66] This is likely also true for the bis(2-(3,5-di-*tert*-butylphenyl)indenyl)hafnium dichloride catalyst system reported here. Thus, for these systems it is likely that atactic stereosequences observed in these polymers are not derived from achiral conformations, but rather from populations of catalyst ion pairs where the conformational dynamics are faster than propylene enchainment (Scheme 1). Under conditions where the conformational dynamics are closely comparable to that of enchainment, atactic sequences will be produced when the rate of insertion is slower than isomerization, whereas isotactic stereosequences will be generated under conditions where the rate of insertion is faster than isomerization. In the latter case, if isomerization still takes place on the lifetime of the polymer chain, the isotactic stereoblock sequences will be separated by [mrmm] stereojunctions as the catalyst isomerizes between stereoselective conformations of opposite stereochemistry (Scheme 1).

Scheme 1. Proposed Mechanism of Enchainment for Bis(2-(3,5-di-*tert*-butylphenyl)indenyl)hafnium Catalyst

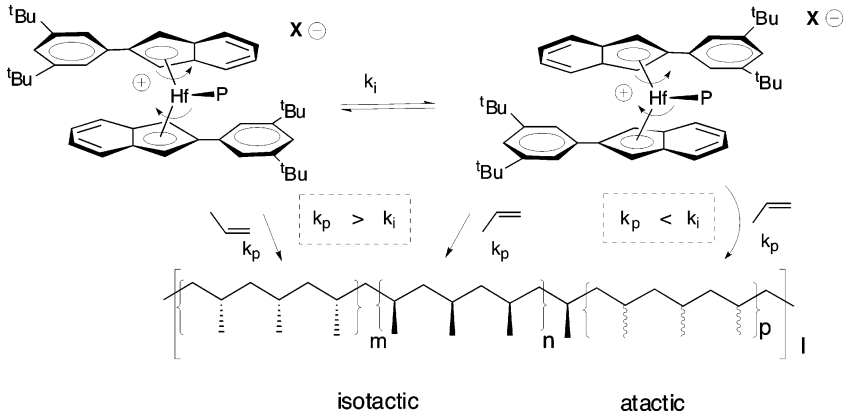

The observed increase in tacticity with increasing molecular weight is also an unusual feature of these catalyst systems. One possible origin of this effect is that the length of the polymer chain influences the rate of conformational isomerism. We think a more likely possibility is that the nature and local conformation of the polymer chain influences the rate of chain transfer. If the rate of β-hydrogen elimination from an atactic chain is faster than that of an isotactic chain, then those populations of catalysts generating atactic chains will be more likely to chain transfer than those generating isotactic chains.

With regard to the compositional heterogeneity, it is not clear that a distribution of isotactic block lengths from a single type of catalyst would yield both the low-tacticity ether-soluble fraction and the highly-isotactic HI fraction, unless the block lengths were on the order of the length of the polymer chain.[45,84] The number and types of stereoerrors indicate that the block lengths are shorter than the polymer chain. Thus, the experimental evidence suggests that activation of these metallocenes generates a population of catalyst sites with different dynamics that leads to compositional heterogeneity, low molecular weight distribution, and a monomer concentration dependence on the stereoselectivity. Further studies with more well-defined activators[58,59] are warranted to test this hypothesis and are the subject of ongoing investigations in our laboratories.

Conclusions

Metallocene catalysts derived from the unbridged bis-(2-(3,5-di-*tert*-butylphenyl)indenyl)hafnium dichloride/MAO yield elastomeric polypropylenes (ePP) of low to intermediate tacticity and low crystallinity. In liquid propylene at 50 °C, this catalyst system yields a polypropylene with $M_w = 201\,000$ and narrow polydispersity ($M_w/M_n = 2.3$) with an average isotacticity [mmmm] = 34%. Despite its narrow polydispersity, the elastomeric polypropylene is heterogeneous as it can be fractionated with boiling-solvent extraction and supercritical fluid fractionations. Solvent extraction yields three fractions increasing in molecular weight, tacticity, and crystallinity: an ether-soluble fraction < a heptane-soluble fraction < a heptane-insoluble fraction. Supercritical fractionations either by molecular weight or crystallinity reveal increasing molecular weight fractions alongside the melting temperatures and the heats of fusion. DSC measurements provide evidence of the presence of long isotactic segments in these otherwise low-tacticity materials. The compositional heterogeneity of these materials suggests that these unbridged metallocenes generate a family of conformationally dynamic catalysts.

Experimental Section

Synthesis of Polypropylene ePP-10. Elastomeric polypropylene (ePP-10) was synthesized by BP Chemical Co. in liquid propylene at 50 °C with the bis(2-(3,5-di-*tert*-butylphenyl)indenyl)hafnium dichloride/MAO catalyst system. The synthesis of this metallocene was previously reported.[75] Propylene (23.6 kg) and heptane (2.7 kg), which were purified by standard column procedures to remove oxygen and water, were charged to a 19 gal (72 L) reactor and stirred while heated to 43 °C. In a drybox, 0.1509 g of catalyst bis(2-(3,5-di-*tert*-butylphenyl)indenyl)hafnium dichloride was dissolved in 50 g of toluene, mixed with 115 g of MAO (11% Al), and transferred to a feed cylinder with 50 mL of additional toluene. After 30 min, the metallocene/MAO solution was added to the reactor. The polymerization temperature was allowed to rise to 50 °C and maintained for 2 h. Pressure was then reduced to atmospheric to flash unreacted propylene, after which toluene was added to dissolve the polymer. The polymer was recovered by coagulation in methanol, washed with water, and air-dried at 65 °C to yield 7.85 kg of elastomeric polypropylene. ^{13}C NMR sequence analysis indicated [m] = 72.9%, [mm] = 54.8%, and [mmmm] = 34.0%. GPC analysis of molecular weight indicated $M_n = 87\,200$ and $M_w = 201\,000$ ($M_w/M_n = 2.3$). The melt flow rate was 10.6 g/10 min at 230 °C with 2.16 kg load.

Fractionation. Solvent boiling extraction was carried out by successive extraction of ePP-10 with boiling diethyl ether and heptane under a nitrogen environment following the procedure reported previously.[45] A 500 mL round-bottom flask attached to a Kumagawa extractor was charge with 300 mL of solvent with 0.2% weight antioxidant 2,6-di-*tert*-butyl-4-methylphenol (BHT). About 10 g of polymer was packed into a thimble layered with a plug of glass wool. Extraction was conducted for 24 h with a heating rate such that the flushing frequency of the extractor was 4 min/flush. After the extraction, polymer was precipitated in acidified methanol (3000 mL, 1% HCl) with vigorous stirring. The thimble (with contents) was then dried using an air flush at room temperature between solvent changes. Heptane-insoluble polymer remaining in the thimble was dissolved in xylene and precipitated by pouring into acidified methanol. The extraction was repeated twice for each solvent. The precipitated polymers were then dried in a vacuum for at least 1 day. Table 1 shows the characterization data of the elastomeric polypropylene ePP-10 together with its solvent fractions.

Supercritical fluid fractionation was carried out to fractionate ePP-10 either by size (molecular weight) or by crystallinity.[78,79,85] Fractionation was performed in the presence of antioxidant Irganox 1010 to avoid/minimize polymer degradation. Fractionation by size was carried out by the isothermal increasing pressure profiling (IPP) method at a constant

temperature of 140 °C using supercritical ethane. In the extraction column, 11.50 g of ePP-10 was charged and dispersed over a dense stainless steel knitted mesh. After sealing the vessel was pressurized with ethane above its critical pressure, the temperature was heated to and maintained at 140 °C. The polymer was fractionated isothermally by ramping the pressure from 100 to 700 bar. At each selected pressure level, polymer fraction was collected until there was a drastic drop in the material flow rate. Subsequently, the pressure was raised and the next polymer fraction was extracted. In this fractionation, 12 fractions were collected to a total weight of 11.12 g (recovery of 96.6%). Table 5 shows the characterization of the representative fractions.

Fractionation based on crystallinity was carried out using critical isobaric temperature rising elution fractionation (CITREF).[78,79,85] The fractionation mechanism of CITREF is analogous to temperature rising elution fractionation (TREF).[86] In this method, polymer was charged to the extraction vessel, heated, and pressurized until complete polymer dissolution and uniform concentration took place. Subsequently, the polymer solution was cooled isobarically to produce a thin semicrystalline layer on the support. Fractions with higher crystallization were deposited first, followed by subsequent lower crystallization fractions. Fractionation took place isobarically at 240 bar by increasing the temperature stepwise ranging from 20 to 160 °C. Separation occurred through selective melting of crystalline fractions that were extracted at each temperature range.

CITREF for ePP-10 was carried out on two duplicate fractionations. In the first fractionation, 6.12 g of polymer was dissolved in the vessel at 700 bar and 140 °C in SCF propane. The polymer was crystallized onto the support by decreasing temperatures at a rate of 5 °C/h while maintaining a constant pressure of 700 bar during the decreasing temperature ramp. The pressure was then lowered to 240 bar (which was known to dissolve the high molecular weight isotactic PP), and fractionation of this sample, at isobaric pressure of 240 bar from stepwise increase in temperature between 40 and 120 °C, recovered 6.12 g in nine fractions (Table 6). In the second experiment 5.02 g was precipitated at stepwise temperature decrease from 160 to 20 °C, and fractionation in stepwise temperature increase recovered 5.00 g of polymer in nine fractions; analysis of four of those fractions is reported in Table 6.

Polymer Characterization: Gel Permeation Chromatography (GPC). Molecular weight characterization of ePP-10 and its fractions was obtained using a Waters 150C high-temperature chromatograph. The solvent carrier was 1,2,4-trichlorobenzene at 139 °C at a flow rate of 1 mL/min through two PL GEL Mixed-B columns. Calibration was performed against polypropylene standards. Molecular weight characterization of the acid digested polymers was carried out with a room temperature GPC Waters 410 using tetrahydrofuran as the solvent carrier. Elution time calibration was conducted against polystyrene standards.

Nuclear Magnetic Resonance (NMR). Characterization of the stereoconfiguration of polymers was performed with solution ^{13}C NMR using a Varian Inova-300 NMR spectrometer. In a 10 mm NMR tube, 150−200 g of polymer was dissolved in 1,1,2,2,-tetrachloroethane containing 0.5 mL of 1,1,2,2-tetrachloroethane-d_2. ^{13}C spectra were recorded at 75.425 MHz at 100 °C with a spectral and pulse width of 7500 Hz and 28°, respectively, with at least 5000 transients.

Differential Scanning Calorimetry (DSC). Thermal analysis was performed on a Perkin-Elmer 7 differential scanning calorimeter using indium as calibration standard. Polymer samples were melt-pressed between two Teflon sheets at 180 °C using light pressure (≤250 psig). Disklike samples were punched from liquid N_2 quenched film using a standard single-hole paper puncher. Samples (5−15 mg) were weighed and sealed into Perkin-Elmer aluminum DSC pans. All samples were initially preheated to 200 °C with a rate of 40 °C/min and held at 200 °C for 5 min. For regular DSC analysis, samples were cooled from 200 °C to room temperature at 20 °C/min and aged at room temperature for 24 h. After aging, samples were cooled to −25 °C at 20 °C/min and held for 5 min before endotherm scans were performed. For thermal fractionation analysis, samples were cooled from 200 to 160 °C at 40 °C/min; then samples were annealed for 12 h at 10 °C intervals to a final temperature of 50 °C. Melting points (T_m, peak of endotherm curve) and heat of fusion (ΔH_f) were measured by heating from −25 to 200 °C with a rate of 20 °C/min. DSC crystallinity was calculated by normalizing the heat of fusion (ΔH_f) from the endotherm scans by the theoretical value of a completely crystalline sample of 209 J/g.[87]

Thermal annealing of elastomeric polypropylene was carried out in a vacuum oven with a compression-molded ePP-10 sample. The sample was annealed at 160 °C for 1 day, 155 °C for 1 day, and 150 °C for 1 day. Then, the sample was cooled to room temperature in 10 °C increments and held for 12 h at each temperature. The temperature was controlled by adjusting the voltage regulator on the vacuum oven and monitoring the internal temperature with a thermometer.

Infrared Spectroscopy (IR). Infrared analysis was performed using a Perkin-Elmer 1600 series FT-infrared spectrometer. Melt-pressed polymer films were allowed to stand overnight at room temperature prior to analysis. Polymer films were scanned from 1600 to 450 cm^{-1} with a resolution of 2 cm^{-1}. Absorbance intensities of the peaks centered at 998 and 975 cm^{-1} were measured, and the ratio of these two peak intensities was calculated as the IR index (A_{998}/A_{975}).

Acknowledgment. G.G.F., R.M.W., and W.W. acknowledge the National Science Foundation (DMR-9910386, CHE-0305436) for financial support. Z.R.C. acknowledges financial support from BP Chemical Co. We thank BP Chemical Co. for providing the elastomeric polypropylene sample, the molecular weight data, and fruitful discussions.

References and Notes

(1) Dahlmann, M.; Erker, G.; Nissinen, M.; Froehlich, R. *J. Am. Chem. Soc.* **1999**, *121*, 2820−2828.
(2) Dahlmann, M.; Erker, G.; Bergander, K. *J. Am. Chem. Soc.* **2000**, *122*, 7986−7998.
(3) Scheirs, J., Kaminsky, W., Eds. *Metallocene-Based Polyolefins*; Wiley: Chichester, 2000; Vol. 2.
(4) Lovinger, A. J.; Lotz, B.; Davis, D. D.; Schumacher, M. *Macromolecules* **1994**, *27*, 6603−6611.
(5) Thomann, R.; Kressler, J.; Mulhaupt, R. *Polymer* **1998**, *39*, 1907−1915.
(6) Natta, G.; Pino, P.; Corradini, P.; Danusso, F.; Mantica, E.; Mazzanti, G.; Moraglio, G. *J. Am. Chem. Soc.* **1955**, *77*, 1708−1710.
(7) Natta, G.; Pino, P.; Mazzanti, G.; Longi, P. *Gazz. Chim. Ital.* **1957**, *87*, 570−585.
(8) Natta, G.; Mazzanti, G.; Crespi, G.; Moraglio, G. *Chim. Ind. (Milan)* **1957**, *39*, 275−283.
(9) Natta, G. *J. Polym. Sci.* **1959**, *34*, 531−549.
(10) Natta, G.; Crespi, G. U.S. Patent 3,175,999, 1965.
(11) Collette, J. W.; Ovenall, D. W.; Buck, W. H.; Ferguson, R. C. *Macromolecules* **1989**, *22*, 3858−3866.
(12) Collette, J. W.; Tullock, C. W. U.S. Patent 4,335,225, 1982.
(13) Tullock, C. W.; Tebbe, F. N.; Mulhaupt, R.; Ovenall, D. W.; Setterquist, R. A.; Ittel, S. D. *J. Polym. Sci., Part A: Polym. Chem.* **1989**, *27*, 3063−3081.
(14) Ittel, S. D. *J. Macromol. Sci., Chem.* **1990**, *A27*, 9−11.
(15) Collette, J. W.; Tullock, C. W.; MacDonald, R. N.; Buck, W. H.; Su, A. C. L.; Harrel, J. R.; Mulhaupt, R.; Anderson, B. C. *Macromolecules* **1989**, *22*, 3851−3858.
(16) Tullock, C. W.; Mulhaupt, R.; Ittel, S. D. *Makromol. Chem., Rapid Commun.* **1989**, *10*, 19−23.
(17) Job, R. C.; Haas, D. F. U.S. Patent 5,118,768, 1992.
(18) Chen, R.; Xie, M. R.; Wu, Q.; Lin, S. G. *J. Polym. Sci., Part A: Polym. Chem.* **2000**, *38*, 411−415.
(19) Kuhl, O.; Koch, T.; Somoza, F. B.; Junk, P. C.; Hey-Hawkins, E.; Plat, D.; Eisen, M. S. *J. Organomet. Chem.* **2000**, *604*, 116−125.
(20) Longo, P.; Amendola, A. G.; Fortunato, E.; Boccia, A. C.; Zambelli, A. *Macromol. Rapid Commun.* **2001**, *22*, 339−344.

(21) Mansel, S.; Perez, E.; Benavente, R.; Perena, J. M.; Bello, A.; Roll, W.; Kirsten, R.; Beck, S.; Brintzinger, H. H. *Macromol. Chem., Phys.* **1999**, *200*, 1292−1297.
(22) Nedorezova, P. M.; Tsvetkova, V. I.; Bravaya, N. M.; Savinov, D. V.; Optov, V. A. *J. Polym. Sci., Ser. A* **2000**, *42*, 573−579.
(23) Schmidt, R.; Alt, H. G. *J. Organomet. Chem.* **2001**, *621*, 304−309.
(24) Yoon, J. S.; Lee, Y. S.; Park, E. S.; Lee, I. M.; Park, D. K.; Jung, S. O. *Eur. Polym. J.* **2000**, *36*, 1271−1275.
(25) Resconi, L.; Piemontesi, F.; Lin-Chen, Y. U.S. Patent 5,747,-621, 1998.
(26) Sassmannshausen, J.; Bochmann, M.; Rosch, J.; Lilge, D. *J. Organomet. Chem.* **1997**, *548*, 23−28.
(27) Chien, J. C. W.; Llinas, G. H.; Rausch, M. D.; Lin, Y. G.; Winter, H. H.; Atwood, J. L.; Bott, S. G. *J. Polym. Sci., Part A: Polym. Chem.* **1992**, *30*, 2601−2617.
(28) Mallin, D. T.; Rausch, M. D.; Lin, Y. G.; Dong, S.; Chien, J. C. W. *J. Am. Chem. Soc.* **1990**, *112*, 2030−2031.
(29) Llinas, G. H.; Dong, S. H.; Mallin, D. T.; Rausch, M. D.; Lin, Y. G.; Winter, H. H.; Chien, J. C. W. *Macromolecules* **1992**, *25*, 1242−1253.
(30) Chien, J. C. W.; Llinas, G. H.; Rausch, M. D.; Lin, G. Y.; Winter, H. H.; Atwood, J. L.; Bott, S. G. *J. Am. Chem. Soc.* **1991**, *113*, 8569−8570.
(31) Cheng, H. N.; Babu, G. N.; Newmark, R. A.; Chien, J. C. W. *Macromolecules* **1992**, *25*, 6980−6987.
(32) Gauthier, W. J.; Corrigan, J. F.; Taylor, N. J.; Collins, S. *Macromolecules* **1995**, *28*, 3771−3778.
(33) Gauthier, W. J.; Collins, S. *Macromolecules* **1995**, *28*, 3779−3786.
(34) Bravakis, A. M.; Bailey, L. E.; Pigeon, M.; Collins, S. *Macromolecules* **1998**, *31*, 1000−1009.
(35) Dietrich, U.; Hackmann, M.; Rieger, B.; Klinga, M.; Leskelae, M. *J. Am. Chem. Soc.* **1999**, *121*, 4348−4355.
(36) Kukral, J.; Lehmus, P.; Feifel, T.; Troll, C.; Rieger, B. *Organometallics* **2000**, *19*, 3767−3775.
(37) Pellon, B. J.; Allen, G. C. Eur. Pat. Appl. 0 475 306 A1, 1992.
(38) Coates, G. W.; Waymouth, R. M. *Science* **1995**, *267*, 217−219.
(39) Hauptman, E.; Waymouth, R. M.; Ziller, J. W. *J. Am. Chem. Soc.* **1995**, *117*, 11586−11587.
(40) Bruce, M. D.; Coates, G. W.; Hauptman, E.; Waymouth, R. M.; Ziller, J. W. *J. Am. Chem. Soc.* **1997**, *119*, 11174−11182.
(41) Kravchenko, R.; Masood, A.; Waymouth, R. M. *Organometallics* **1997**, *16*, 3635−3639.
(42) Petoff, J. L. M.; Bruce, M. D.; Waymouth, R. M.; Masood, A.; Lal, T. K.; Quan, R. W.; Behrend, S. J. *Organometallics* **1997**, *16*, 5909−5916.
(43) Bruce, M. D.; Waymouth, R. M. *Macromolecules* **1998**, *31*, 2707−2715.
(44) Carlson, E. D.; Krejchi, M. T.; Shah, C. D.; Terakawa, T.; Waymouth, R. M.; Fuller, G. G. *Macromolecules* **1998**, *31*, 5343−5351.
(45) Hu, Y. R.; Krejchi, M. T.; Shah, C. D.; Myers, C. L.; Waymouth, R. M. *Macromolecules* **1998**, *31*, 6908−6916.
(46) Kravchenko, R.; Masood, A.; Waymouth, R. M.; Myers, C. L. *J. Am. Chem. Soc.* **1998**, *120*, 2039−2046.
(47) Kravchenko, R.; Waymouth, R. M. *Macromolecules* **1998**, *31*, 1−6.
(48) Lin, S.; Hauptman, E.; Lal, T. K.; Waymouth, R. M.; Quan, R. W.; Ernst, A. B. *J. Mol. Catal. A: Chem.* **1998**, *136*, 23−33.
(49) Petoff, J. L. M.; Agoston, T.; Lal, T. K.; Waymouth, R. M. *J. Am. Chem. Soc.* **1998**, *120*, 11316−11322.
(50) Witte, P.; Lal, T. K.; Waymouth, R. M. *Organometallics* **1999**, *18*, 4147−4155.
(51) Carlson, E. D.; Fuller, G. G.; Waymouth, R. M. *Macromolecules* **1999**, *32*, 8100−8106.
(52) Carlson, E. D.; Fuller, G. G.; Waymouth, R. M. *Macromolecules* **1999**, *32*, 8094−8099.
(53) Hu, Y. R.; Carlson, E. D.; Fuller, G. G.; Waymouth, R. M. *Macromolecules* **1999**, *32*, 3334−3340.
(54) Lin, S.; Waymouth, R. M. *Macromolecules* **1999**, *32*, 8283−8290.
(55) Petoff, J. L. M.; Myers, C. L.; Waymouth, R. M. *Macromolecules* **1999**, *32*, 7984−7989.
(56) Tagge, C. D.; Kravchenko, R. L.; Lal, T. K.; Waymouth, R. M. *Organometallics* **1999**, *18*, 380−388.
(57) Waymouth, R. M.; Hauptman, E.; Coates, G. W. U.S. Patent 5969070, 1999.
(58) Wilmes, G. M. L. S. L.; Ernst, E. B.; Waymouth, R. M. *Macromolecules* **2002**, *35*, 5382−5387.
(59) Wilmes, G. M.; Polse, J. L.; Waymouth, R. M. *Macromolecules* **2002**, *35*, 6766−6772.
(60) Schoenherr, H.; Wiyatno, W.; Pople, J.; Frank, C. W.; Fuller, G. G.; Gast, A. P.; Waymouth, R. M. *Macromolecules* **2002**, *35*, 2654−2666.
(61) Schoenherr, H.; Waymouth, R. M.; Frank, C. W. *Macromolecules* **2003**, *36*, 2412−2418.
(62) Wiyatno, W.; Fuller, G. G.; Pople, J. A.; Gast, A. P.; Chen, Z.-r.; Waymouth, R. M.; Myers, C. L. *Macromolecules* **2003**, *36*, 1178−1187.
(63) Wiyatno, W.; Pople, J. A.; Gast, A. P.; Waymouth, R. M.; Fuller, G. G. *Macromolecules* **2002**, *35*, 8498−8508.
(64) Wiyatno, W.; Pople, J. A.; Gast, A. P.; Waymouth, R. M.; Fuller, G. G. *Macromolecules* **2002**, *35*, 8488−8497.
(65) Busico, V.; Cipullo, R.; Segre, A. L.; Talarico, G.; Vacatello, M.; Castelli, V. V. A. *Macromolecules* **2001**, *34*, 8412−8415.
(66) Busico, V.; Cipullo, R.; Kretschmer, W. P.; Talarico, G.; Vacatello, M.; Van Axel Castelli, V. *Angew. Chem., Int. Ed.* **2002**, *41*, 505−508.
(67) Busico, V.; Cipullo, R.; Kretschmer, W.; Talarico, G.; Vacatello, M.; Castelli, V. V. *Macromol. Symp.* **2002**, *189*, 127−141.
(68) Busico, V.; Castelli, V. V. A.; Aprea, P.; Cipullo, R.; Segre, A.; Talarico, G.; Vacatello, M. *J. Am. Chem. Soc.* **2003**, *125*, 5451−5460.
(69) Madkour, T. M.; Mark, J. E. *Polymer* **1998**, *39*, 6085−6091.
(70) Madkour, T. M.; Mark, J. E. *Macromol. Theory Simul.* **1998**, *7*, 69−77.
(71) Bensason, S.; Stepanov, E. V.; Chum, S.; Hiltner, A.; Baer, E. *Macromolecules* **1997**, *30*, 2436−2444.
(72) Bensason, S.; Minick, J.; Moet, A.; Chum, S.; Hiltner, A.; Baer, E. *J. Polym. Sci., Part B: Polym. Phys.* **1996**, *34*, 1301−1315.
(73) Bensason, S.; Nazarenko, S.; Chum, S.; Hiltner, A.; Baer, E. *Polymer* **1997**, *38*, 3513.
(74) Lin, S.; Waymouth, R. M. *Acc. Chem. Res.* **2002**, *35*, 765−773.
(75) Dankova, M.; Waymouth, R. M. *Macromolecules* **2003**, *36*, 3815−3820.
(76) We did not analyze the samples carefully for regioerrors as samples from similar catalysts show less than 1% regioerrors (ref 54).
(77) Kravchenko, R.; Sauer, B. B.; McLean, R. S.; Keating, M. Y.; Cotts, P. M.; Kim, Y. H. *Macromolecules* **2000**, *33*, 11−13.
(78) Britto, L. J. D.; Soares, J. B. P.; Penlidis, A.; Krukonis, V. *J. Polym. Sci., Part B: Polym. Phys.* **1999**, *37*, 553−560.
(79) McHugh, M.; Krukonis, V. *Supercritical Fluid Extraction*, 2nd ed.; Butterworth-Heinemann: Boston, 1994.
(80) Balboni, D.; Moscardi, G.; Baruzzi, G.; Braga, V.; Camurati, I.; Piemontesi, F.; Resconi, L.; Nifant'ev, I. E.; Venditto, V.; Antinucci, S. *Macromol. Chem., Phys.* **2001**, *202*, 2010−2028.
(81) Auriemma, F.; De Rosa, C.; Boscato, T.; Corradini, P. *Macromolecules* **2001**, *34*, 4815.
(82) Statistical analysis of HS-ePP10 by Bernoullian statistics yields a $P(m)$ of 0.815 with a weighted error of 2.436, whereas the two-site Chujo model yields $w = 0.198$, $\sigma = 0.813$, and $\alpha = 0.854$ with a weighted error of 0.314, where w is the mole fraction of sequences under enantiomorphic site control, α is the probability of a stereoselective insertion at the enantiomorphic site, and σ is the probability of a *meso* insertion at the Bernoullian site. Similar analysis for IPP-11: Bernoullian $P(m) = 0.785$; weighted error = 5.518. Two-site: $w = 0.198$, $\sigma = 0.691$, and $\alpha = 1.00$ with a weighted error of 0.540 (refs 43 and 45).
(83) Busico, V.; Cipullo, R. *Prog. Polym. Sci.* **2001**, *26*, 443−533.
(84) Nele, M.; Collins, S.; Dias, M. L.; Pinto, J. C.; Lin, S.; Waymouth, R. M. *Macromolecules* **2000**, *33*, 7249−7260.
(85) Folie, B.; Kelchtermans, M.; Schutt, J. R.; Schonemann, H.; Krukonis, V. *J. Appl. Polym. Sci.* **1997**, *64*, 2015−2030.
(86) Xu, J.; Feng, L. *Eur. Polym. J.* **2000**, *36*, 867−878.
(87) Wunderlich, B. *Macromolecular Physics;* Academic Press: New York, 1976; Vol. 2.

MA020332J